Donor−Acceptor Diblock Copolymers Based on PPV and C_{60}: Synthesis, Thermal Properties, and Morphology

Marleen H. van der Veen,[†] Bert de Boer,*[,†] Ulf Stalmach, Karin I. van de Wetering,[‡] and Georges Hadziioannou[‡]

Department of Polymer Chemistry, Materials Science Centre, University of Groningen, Nijenborgh 4, NL-9747 AG, Groningen, The Netherlands

Received October 31, 2003; Revised Manuscript Received February 27, 2004

ABSTRACT: An improved synthetic method to nitroxide end-capped poly(*p*-phenylenevinylene)s is presented. The nitroxide-functionalized PPVs are extended with a second coillike block by employing them as macroinitiators in a nitroxide-mediated radical polymerization (NMRP) of monomers like styrene, 4-chloromethylstyrene, 4-vinylpyridine, and *n*-butyl acrylate. The observed thermotropic properties and morphology of films based on the rod−coil diblock copolymers are identified and described. Some of the block copolymers are subsequently subjected to a coupling with C_{60} to incorporate electron-accepting properties into these PPV-based diblock copolymers. For this, a statistical copolymer built from styrene and azidomethylstyrene was used as the second coillike block, making it possible to *adjust* the built-in ratio of C_{60}. The morphology and thermotropic properties of films prepared with these diblock copolymers are investigated.

Introduction

The advantage offered by polymers over the traditional semiconductor materials is the low cost and versatility of processing methods, which allows the polymer film to attain virtually any desired shape. Casting a thin film over a macroscopically large area is feasible and particularly attractive when reducing the processing costs. For this to become reality the parent-conjugated polymers, which are often intractable because of their stiff backbone, have to be derivatized without deterioration of their optoelectronic properties. Besides the molecular structure, details of the processing history could play a key role in determining the properties and morphology of such polymeric materials. Therefore, each step has to be carefully carried out and studied in detail when aiming at controlled properties of thin polymer films.

The majority of publications on conjugated polymers and their applications describe polymers based on poly(1,4-phenylenevinylene) (PPV) that were synthesized by a precursor route (Gilch,[1] Wessling and Zimmerman,[2] etc.), Heck coupling,[3] Wittig[4] (−Horner)[5] condensation, McMurry coupling,[6] etc.[7] These methods yield high molecular weight polymers with a high content of the desired trans double bonds such as for example poly[2-methoxy-5-(2′-ethylhexyloxy)-1,4-phenylenevinylene] (MEH−PPV), poly[2-methoxy-5-(3′,7′-dimethyloctyloxy)-1,4-phenylenevinylene] (MDMO−PPV), and poly[(2,5-dioctyloxy)-1,4-phenylenevinylene] (DOO−PPV) or its analogue DEH−PPV with 2,5-di(2′-ethyl)hexyloxy as side chains. Unfortunately, most PPVs exhibit a high polydispersity (PD), making them less applicable to control the morphology in the solid state. Moreover, the end-group functionality cannot be controlled exactly by one of these methods, and the nature of the end groups is difficult to determine due to their high molecular weight. We aim to control the end groups and modify them to obtain diblock copolymers with a well-defined structure. This can be accomplished in two different ways. One approach is the synthesis of well-defined conjugated oligomers,[8−10] in which one has the advantage of controlling the end groups and the molecular weight exactly. Such a multistep route is rather time-consuming when aiming at higher molecular weights. Our approach is based on a second method: the one-step synthesis of conjugated polymers with relatively high, *controllable* molecular weight (around or above the effective conjugation length) and a relatively low PD.[11] The PPV-based homopolymers reported in this paper do contain exactly one end group per chain, which can be modified to obtain a macroinitiator for nitroxide-mediated radical polymerization (NMRP).

Conjugated polymers can be regarded as (rigid) rodlike systems with restricted flexibility compared to conventional polymers like polystyrene (coillike). This may result in complex phase behavior for diblock copolymers containing at least one conjugated block. The presence of such a stiff block puts these diblock copolymers in the class of rod−coil diblock copolymers.[12,13] The rodlike block may be the liquid-crystal-forming segment or so-called mesogen,[14−16] which plays an important role during the microphase separation. Block copolymers that contain such liquid-crystalline segments have several thermal transitions, namely, a glass transition temperature for each distinct block, a phase transition temperature for the liquid-crystalline block, and the order−disorder transition temperature. They may give rise to an enhanced microphase separation[14,17] and morphologies distinctly different from the conventional spheres, cylinders, or lamellar structures,[18] which may include arrowhead, zigzag, and wavy lamellae phases.[14,15] Stupp and co-workers showed that even low molecular weight rod−coil block copolymers can microphase separate in highly ordered phases as a consequence of a larger Flory−Huggins interaction parameter (χ).[19−21] In

[†] Present address: Molecular Electronics, University of Groningen.

[‡] Present address: Ecole Européenne de Chimie, Polymères Matériaux (ECPM), Universitè Louis Pasteur Strasbourg, 25, rue Becquerel, F-67087 Strasbourg Cedex 2, France.

* To whom correspondence should be addressed: e-mail b.de.boer@phys.rug.nl.

10.1021/ma035643o CCC: $27.50
Published on Web 04/21/2004

related studies by Yu and co-workers, the well-defined rod−coil block copolymers based on substituted PPVs and poly(isoprene) (PI),[9] poly(methyl methacrylate) (PMMA),[22] or poly(ethylene oxide) (PEO) formed liquid-crystalline phases which comprise the substituted PPV.[10,23] As in the work of Stupp and co-workers, low-molecular-weight hairy-rod blocks were used, and the microphase separation obtained suggests strong mutual interactions of the liquid-crystalline blocks. Additional results presented in our previous work[24,25] have demonstrated that changes in the thermodynamics of the environment result in quite complex and yet unexplored behavior of the rod−coil diblock copolymers in solution. These forms of self-organization are likely to act as the "nuclei" for solidification and will bring about the morphology of the solid film obtained under certain processing conditions. Thermal treatment of, for example, a film of MEH−PPV was found to improve the device efficiency of diodes, which was attributed to a higher degree of interchain interaction.[26,27] An enhanced ordering of the microstructure is generally obtained through annealing, both in homopolymers and in conventional block copolymers. Likewise, thermal treatment of films of rod−coil block copolymers results in an enhanced ordering of the microphase-separated morphology.[9]

On the basis of the reported thin film properties, it appears advantageous to be able to correlate the morphology with the optoelectronic properties. The device performance depends on the balance between intrachain and interchain electronic interactions. Hence, the morphology of the thin polymer film plays an important role in determining the optoelectronic properties of light-emitting diodes (LEDs) and photovoltaic (PV) cells. In PV cells, the combination of a poly(*p*-phenylenevinylene)-type polymer as the donor (D) material and C_{60} as acceptor (A) has proven promising.[28] Materials that combine the physical properties of fullerene and the processability of polymers can be obtained by covalently connecting the C_{60} to the polymer.[25,29] The PPV-based diblock copolymers reported in this paper have a controlled amount of C_{60} and are used in a systematic study to correlate the morphology and processing conditions to, ultimately, the device performance.

Results and Discussion

NMRP Copolymerization with PPV-Based Macroinitiators. The DEH−PPV homopolymer was synthesized via the Siegrist polycondensation of **1** (Scheme 1), which is originally described by Kretzschmann et al.[30] This condensation via a Schiff base results in a narrow molecular weight distribution and exactly one terminal aldehyde group per chain.[24,25,31] To obtain the NMRP macroinitiator, the aldehyde end group of the low-molecular-weight polymer ($M_n = 7.9 \times 10^3$ g/mol for DEH−$PPV_{k=21}$) is converted to an alkoxyamine based on TIPNO (Scheme 2).

Both syntheses published in the literature for the comparable DOO−PPV macroinitiator, either via a Grignard reagent[25] or via an organolithium compound,[31] could not be repeated successfully. The in situ formed lithiated anion (generated from **2**) is therefore converted into the more stable Grignard reagent by reaction with $MgBr_2$ (transmetalation). A large excess of **3** guarantees a complete conversion of the aldehyde group (Scheme 2). This improved procedure for the synthesis of the NMRP macroinitiator, which is a combination of the previously reported methods, was found to be very reproducible. The formation of the DEH−PPV−TIPNO macroinitiator is easily visualized by the disappearance of the aldehyde signal at 10.4 ppm in the ^{1}H NMR spectrum and the emergence of a signal at 5.9 ppm from the −C*H*(OH)− group.

Scheme 1. Synthesis of the DEH−PPV Homopolymer (Siegrist Condensation) and the Transmetalation of the TIPNO Linker[a]

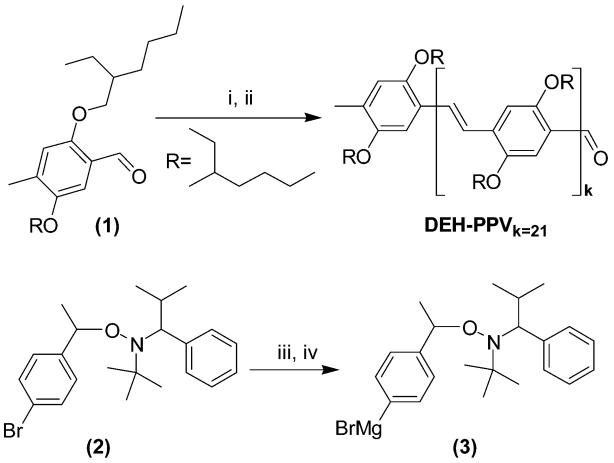

[a] (i) Aniline, 60 °C, 1 h; (ii) KOtBu, DMF, 80 °C, 3 h; (iii) *t*-BuLi, ether, −78 °C; (iv) $Br_2Mg{\cdot}OEt_2$, ether, RT.

The macroinitiator DEH−PPV−TIPNO is chain extended with a statistical copolymer of styrene (S) and 4-chloromethylstyrene (CMS, Scheme 2). To estimate the chain growth in time of the diblock copolymer, samples were taken during the NMRP copolymerization with DEH−$PPV_{k=15}$−TIPNO (Table 1). The monomer conversions were kept below 25% to ensure a low viscosity of the reaction mixture. The monomer composition as well as the chain length of the P(S-*stat*-CMS) was determined using ^{1}H NMR spectroscopy, assuming that the DEH−PPV block remains unchanged. The nature of the copolymerization is elucidated in a plot of the molecular weight of the growing P(S-*stat*-CMS) block (M_{nPS}) vs time (Figure 1). Using the DEH−$PPV_{k=15}$−TIPNO macroinitiator, a linear growth in time and low polydispersities (Table 1) are observed, confirming the "living" character of the NMRP copolymerization. The values of the comonomer composition given in Table 1 clearly illustrate that the determined built-in ratio of the respective monomers is lower than the feed ratio. This is most likely due to the slightly higher reactivity ratio of the CMS comonomer, resulting in a preference to add CMS instead of S. To determine whether the same "living" behavior is observed for a macroinitiator bearing a longer DEH−PPV block, two additional copolymerizations in separated batches were performed with DEH−$PPV_{k=21}$−TIPNO (Table 1, Figure 1). Working with the same relative amount of initiator, Ac_2O, free TIPNO, and the same total amount of monomer (but with a different feed ratio), we diluted the system twice by adding an equal amount of solvent (relative to the total amount of monomer in the system). In doing so, the concentrations of all components were twice as low compared to the bulk copolymerization with DEH−$PPV_{k=15}$−TIPNO. Although we did not investigate the growth in time of these copolymerizations, the NMRP systems with DEH−$PPV_{k=21}$−TIPNO are regarded as being "living" because the combined results are in line with the bulk polymerization of DEH−

Scheme 2. Synthetic Route to Donor−Acceptor Diblock Copolymers via NMRP with the DEH−PPV (Donor) Macroinitiator and Subsequent C_{60} Functionalization (Acceptor) of the Second Copolymer Block[a]

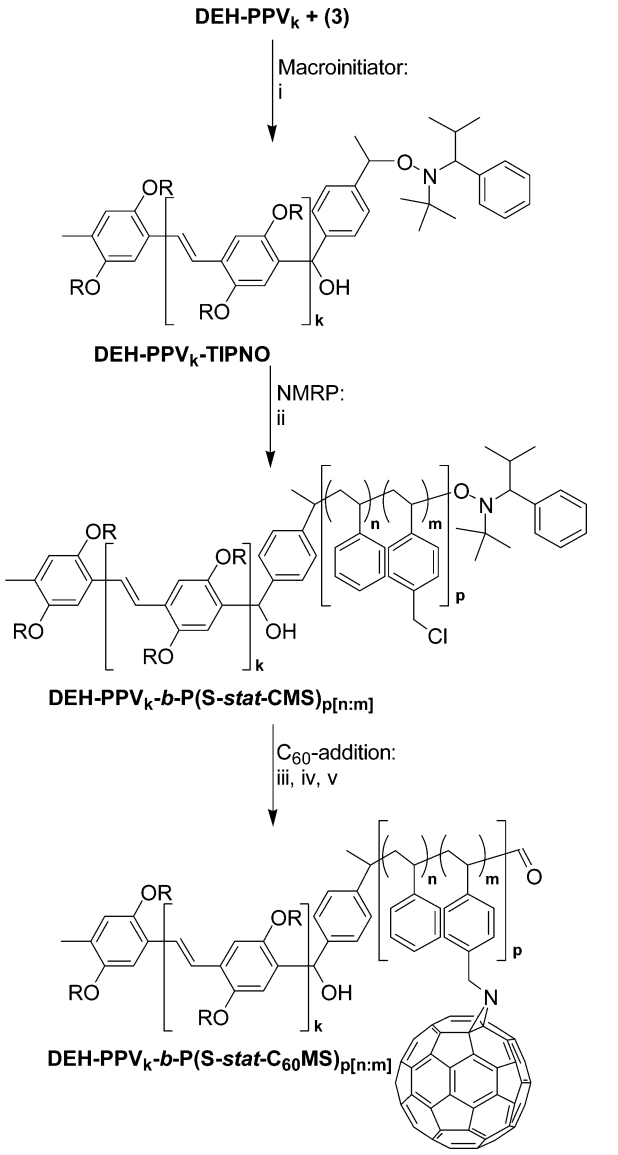

[a] (i) Ether, 35 °C, 16 h; (ii) styrene, 2-chloromethylstyrene, Ac_2O, cat. TIPNO, anisole, 125 °C, 50 min; (iii) NaN_3, DMF, 130 °C, 16 h; (iv) C_{60}, chlorobenzene, 60 °C, 20 h; (v) 130 °C, 1 h.

$PPV_{k=15}$−TIPNO (Table 1). While the monomer concentration has been lowered compared to this bulk copolymerization, no significant reduction of the propagation rate is observed during these copolymerizations. As expected, the monomer built-in ratio of the copolymers prepared with DEH−$PPV_{k=21}$−TIPNO macroinitiator is lower than the feed ratio. Fortunately, it is still possible to adjust and control the monomer composition in the resulting copolymers.

In addition to ^{1}H NMR as characterization method, UV−vis spectroscopy can be used to estimate the relative amount of P(S-*stat*-CMS) in diblock copolymers. Upon chain extension of the DEH−PPV block, its weight-normalized absorbance decreases with increasing P(S-*stat*-CMS) block length. This relative decrease in absorption is related to the weight percentage (wt %) of P(S-*stat*-CMS) incorporated in the diblock copolymer (Table 2). The results obtained with UV−vis spectroscopy are consistent with those values obtained via ^{1}H NMR spectroscopy. Note that the copolymer composition can only be determined by ^{1}H NMR. Alternatively, the P(S-*stat*-CMS) block lengths may be determined by means of GPC. However, this technique is only used to determine the PD (Table 1) since it is not appropriate for an absolute molecular weight determination when rigid-rod-like polymers are involved.

Functionalization of (Di)block Copolymers with C_{60}. It is our objective to incorporate both the donor (D) and acceptor (A) functionalities into one macromolecule by functionalizing our PPV-based diblock copolymers with C_{60}. During this third step toward D−A diblock copolymers the C_{60} is attached to the well-defined statistical P(S-*stat*-CMS) block via the chloromethyl groups (Scheme 2).

Previously, the multifunctional P(S-*stat*-CMS) block had been functionalized with C_{60} by employing atom transfer radical addition (ATRA).[25] This approach has proven to be successful. For example, DOO−$PPV_{k=7}$-*b*-P(S-*stat*-C_{60}MS)$_{19K[1.5:1]}$ containing an average of 15 C_{60} molecules per chain was obtained via this method. Unfortunately, material that is not sufficiently soluble was obtained after employing ATRA. Several research groups use ATRA to graft more than one monofunctional polystyrene chain onto C_{60} yielding dendritic or starlike macromolecules.[32] A chlorine−C_{60} bond is left behind after the addition of a polystyrene chain onto C_{60}. This chlorine bond is less stable than the one of the CMS in our P(S-*stat*-CMS) copolymers, resulting in a high concentration of "polystyrene-C_{60} radicals" during the course of ATRA. Their recombination with other polystyrene-like radicals is very likely. Since we use multifunctional polystyrenic chains, the occurrence of intra- and intermolecular cross-linking (multiadditions onto C_{60}) is very likely. The probability of intramolecular cross-linking has been lowered through systematic "dilution" of the reactive CMS groups with styrene moieties (i.e., higher S:CMS built-in ratio). However, the intermolecular cross-linking is hard to overcome by optimization of all reaction parameters when working with radicals as intermediates. Hawker et al. modified the P(S-*stat*-CMS) copolymers with an azide group to perform a cycloaddition to C_{60} and obtained soluble polymers.[33] The azidomethyl-substituted polystyrene (the so-called "azide intermediate", in our case DEH−PPV-*b*-P(S-*stat*-N_3MS)) reacts in this method with an equimolar amount of C_{60} to yield triazoline **4** (Scheme 3). The thermal extrusion of nitrogen from this triazoline leads to the formation of aza-bridged fullerenes **5** and **6** (and maybe their bisadducts) referred to as bridged iminofullerenes. These fullerenes can have a bridge between five- and six-membered rings and between two six-membered rings (called [5,6]-bridged and [6,6]-bridged, respectively).[34,35] In addition, the isomers may either have closed or open transannular bonds.[36] Of the possible Kekulé structures of C_{60} the ones that have the energetically most favorable arrangement contain exclusively [6,6] double bonds and [5,6] single bonds. So far, and consistent with this "rule", the closed [6,6]-bridged monoadduct (analogous to **5**) and open [5,6]-bridged monoadduct (analogous to **6**) have been observed by Prato et al.[35] The number of π-electrons remains unchanged in the case of the open [5,6]-bridge monoadducts.[29] Recently reported (cyclic voltammetric) data of some polymeric fullerene derivatives confirmed

Table 1. Diblock Copolymers Obtained with NMRP Copolymerization of S and CMS Using DEH−PPV Macroinitiators

	DEH−PPV$_{k=15}$−TIPNO					DEH−PPV$_{k=21}$−TIPNO			
	single batch					batch 1		batch 2	
time (min)	0	40	100	120	140	0	50	0	80
feed[a]	4.0	4.0	4.0	4.0	4.0	3.2	3.2	3.6	3.6
built-in[a]		3.7	3.0	3.0	3.0		2.1		2.6
M_n (kg/mol)[b]	6.1	22.5	52.1	63.4	71.4	8.2	22.4	8.2	38.8
PD	1.2	1.2	1.7	1.8	2.2	1.2	1.5	1.2	1.8

[a] Comonomer S:CMS ratio. [b] Including the TIPNO end group.

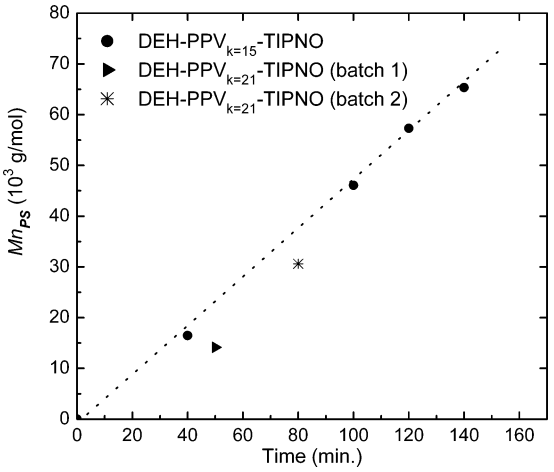

Figure 1. Polymer chain growth in time during NMRP copolymerization of S and CMS with DEH−PPV$_k$−TIPNO macroinitiators.

that the electronic properties indeed resemble those of pristine C_{60}.[37] Therefore, we expect that the C_{60} moieties will still serve as electron acceptor when incorporated into the DEH−PPV-*b*-P(S-*stat*-CMS) diblock copolymers.

The conversion of P(S-*stat*-CMS) copolymers (used as a reference compound) to the corresponding azide intermediate is a versatile method with yields varying from 70 to 85%. The chlorine group is completely converted to an azide when a large excess of NaN_3 is used. Both the preparation of DEH−PPV$_{k=21}$-*b*-P(S-*stat*-N_3MS)$_{14K[2.1:1]}$ and of the reference compound P(S-*stat*-N_3MS)$_{21K[2:1]}$ is easily monitored by ^{1}H NMR and IR spectroscopy. The methylene proton peak of the P(S-*stat*-CMS) copolymers shifts from 4.46 to 4.17 ppm, which is in agreement with the ^{1}H NMR data reported by Ederlé and Mathis.[38] The covalent bond connecting the TIPNO group to DEH−PPV-*b*-P(S-*stat*-CMS) dissociates in radicals due to the high temperature of this conversion (i.e., just as it does during NMRP). The loss of the TIPNO group is confirmed by the absence of its characteristic ^{1}H NMR shift at 0.45 ppm. Moreover, a small aldehyde signal at 10.41 ppm indicates a possible formylation of this radical chain end. The second method used to detect the azide intermediate is IR spectroscopy. The intermediate possesses a strong characteristic band for the azide group at 2094 cm^{-1}. The complete disappearance of this band after cycloaddition to C_{60} confirms the completion of the reaction. The formation of the azide and its subsequent functionalization with C_{60} are both monitored with IR spectroscopy. Convenient methods to determine the covalent bonding of C_{60} and the amount of C_{60}, like ^{1}H NMR spectroscopy, could only be used to observe the structural changes after functionalization with C_{60}. The P(S-*stat*-C_{60}MS)$_{[2:1]}$ reference compounds as well as the DEH−PPV$_{k=21}$-*b*-P(S-*stat*-C_{60}MS)$_{[2.1:1]}$ diblock copolymers are, after complete drying, not sufficiently soluble in common organic solvents like chloroform and chlorobenzene. Nonetheless, a ^{1}H NMR spectrum of DEH−PPV$_{k=21}$-*b*-P(S-*stat*-C_{60}MS)$_{[2.1:1]}$ that contained a minimum amount of dissolved product clearly demonstrated that the signal of the azide intermediate at 4.17 ppm disappeared after reaction with C_{60}. In addition, a characteristic C_{60} absorption peak around 330 nm is clearly present in UV−vis spectra of the filtered solutions (see Supporting Information). Both observations seem to be an indication of the covalent attachment of C_{60} to the polymer.

Other techniques to determine the amount of C_{60} in polymers are DSC and TGA.[25] The latter one is a convenient method when dealing with poorly soluble materials like our DEH−PPV-*b*-P(S-*stat*-C_{60}MS). Figure 2 shows the TGA thermograms of the starting polymers, C_{60}-functionalized polymers, and pristine C_{60}. The molecular weights given for the P(S-*stat*-CMS) block functionalized with C_{60} are their *theoretical* values (i.e., assuming 100% conversion of azide to C_{60}). Diblock copolymers with the same copolymer composition ([*n*:*m*]) are prepared from the same starting materials. In the DEH−PPV-*b*-P(S-*stat*-C_{60}MS) and P(S-*stat*-C_{60}MS) samples, the polymer backbone starts to decompose at 300 °C, leaving a C_{60} adduct which shows only minor weight loss up to 600 °C. This decomposition of the backbone is nearly complete at 550 °C (see the corresponding reference compounds), and we can assume that the residue difference at 575 °C corresponds to the C_{60} content. This residue was thought not to be unreacted C_{60} given that these polymers are dissolved and filtered twice in THF (solubility of C_{60} in THF is <0.01 mg/mL at RT).[39] The P(S-*stat*-CMS)$_{21K[2:1]}$ can contain a (theoretical) maximum amount of 68 wt % of C_{60} after a complete conversion, which would result in P(S-*stat*-C_{60}MS)$_{63K[2:1]}$. A value of 55 wt % C_{60} is found with the TGA analysis indicating that 80% of the theoretical amount is incorporated, giving P(S-*stat*-C_{60}MS)$_{54K[2:1]}$. Higher amounts of C_{60} are found upon increasing the reaction time. Almost 90% of the theoretical value is incorporated when going from 16 to 20 h and using only 1 equiv of C_{60}. However, the yields of the reactions are rather low (about 25%). Yields of about 40% are obtained with DEH−PPV-*b*-P(S-*stat*-C_{60}MS) diblock copolymers when 2 equiv of C_{60} was used.

The synthesized DEH−PPV-*b*-P(S-*stat*-C_{60}MS) diblock copolymers contain 41 and 57 wt % of C_{60} (Figure 2). The latter one with a higher fraction of chloromethyl groups in the starting material indeed gives rise to a higher amount of C_{60}. This agrees well with the initial aim that these groups will determine the C_{60} content in diblock copolymers. A similar trend has already been observed in using ATRA as C_{60} functionalization method.[25] Although the above-presented results are promising, a new problem arises. It seems that after drying the product renders insoluble. Only samples that have not been completely dried could be redissolved.

Table 2. Determination of the P(S-*stat*-CMS) Amount in Diblock Copolymers

		^{1}H NMR spectroscopy			UV−vis spectroscopy	
	NMRP time (min)	total M_n[a]	calcd M_n[a] P(S-*stat*-CMS)	calcd wt % P(S-*stat*-CMS)	absorbance (Abs/mg g^{-1})[c]	calcd wt % P(S-*stat*-CMS)
DEH−PPV$_{k=21}$	0	8.2[b]			54.5	
DEH−PPV$_{k=21}$-*b*-P(S-*stat*-CMS)	50	22.4	14.1	63	19.7	64
DEH−PPV$_{k=21}$-*b*−P(S-*stat*-CMS)	80	38.8	30.6	79	12.4	77

[a] In kg/mol. [b] Including the TIPNO end group. [c] At λ_{max} = 496 nm.

Scheme 3. Cycloaddition of Azide Intermediate DEH−PPV-*b*-P(S-*stat*-N$_3$MS) to C_{60} with Subsequent the Nitrogen Extrusion from the Triazoline Intermediate[a]

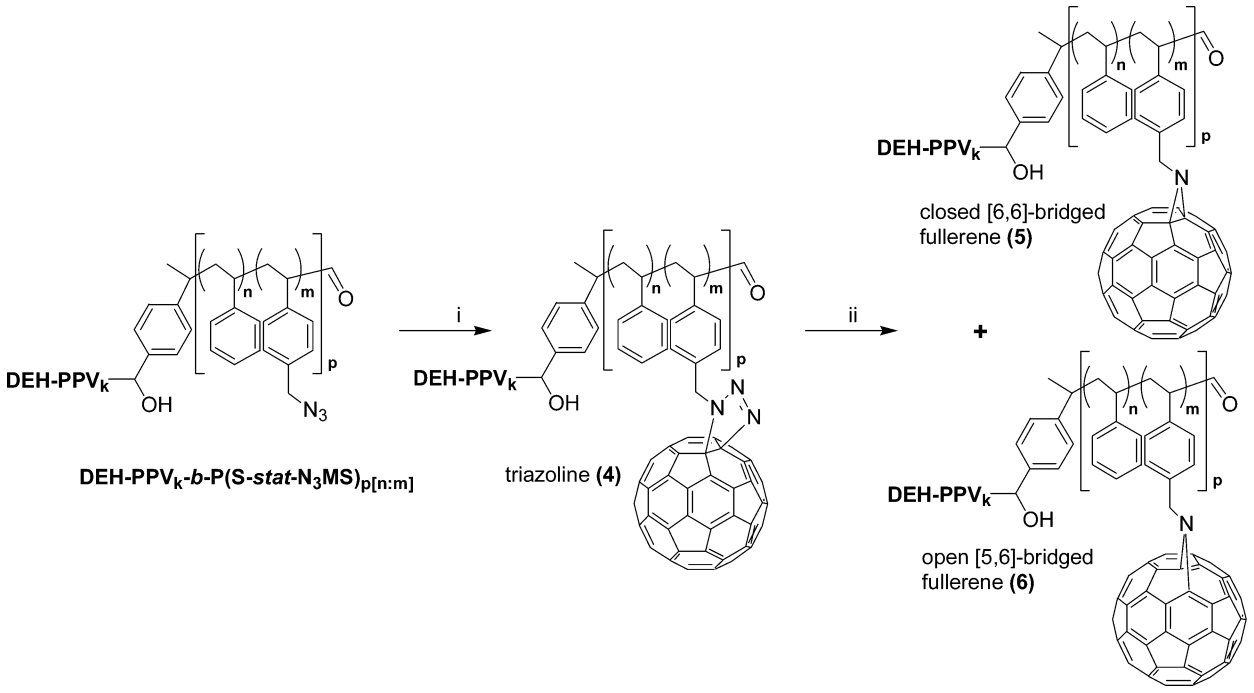

[a] (i) C_{60}, chlorobenzene, 60 °C, 20 h; (ii) chlorobenzene, 130 °C, 1 h.

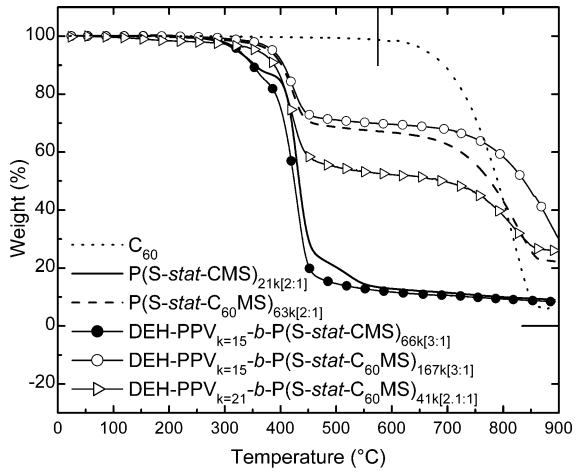

Figure 2. TGA traces of (di)block copolymers recorded under N_2 and a heating rate of 10 °C/min. The amount of residue left at 575 °C represents the wt % C_{60} incorporated. Pristine C_{60} is used as reference compound.

Other groups have observed the same problem, and so far its cause is not clarified.[40] The complete removal of solvents should therefore be avoided during the preparation of these C_{60}-functionalized diblock copolymers.

A significant rise in the T_g of a polystyrenic backbone is expected when the chain stiffness increases due to C_{60} side groups. Therefore, DSC provides qualitative evidence for the incorporation of C_{60} in the polymers. However, no transition temperatures were found in DSC scans of DEH−PPV-*b*-P(S-*stat*-C_{60}MS) diblock copolymers prepared via the azide intermediate. Instead, an enormous exothermic heat flow during the first heating scan is observed (data not given). After this once-only event starting at 80 °C and ending around 220 °C, the samples exhibit no thermal transitions at all in the first cooling scan and the subsequent second heating scan. Further examination with TGA confirms a physical change of the materials: the premature weight loss observed with TGA starting at 120 °C disappears after the sample has been used for a DSC analysis (Figure 3). We hypothesize that the formation of aza-bridged fullerenes is incomplete (the nitrogen extrusion from triazoline **4**, Scheme 3), resulting in exothermic reactions and weight losses. Unfortunately, this hypothesis could not be confirmed with Gibbs energy calculations based on nitrogen extrusion and the total amount of heat released in the first DSC scan. However, the weight loss monitored with TGA seems to match well with a loss of nitrogen during the DSC analysis. The weight percentage of C_{60} in the presented polymer (Figure 3) is 95% of the theoretical amount. Upon thermal extrusion of nitrogen from this polymer the maximum weight loss would be 2.2% while a premature weight loss of 2.1% is found with TGA (difference in residue at 300 °C before and after the DSC scan). These values indicate that the polymer and their intermediate triazolines are not fully converted to aza-bridged fullerenes during the

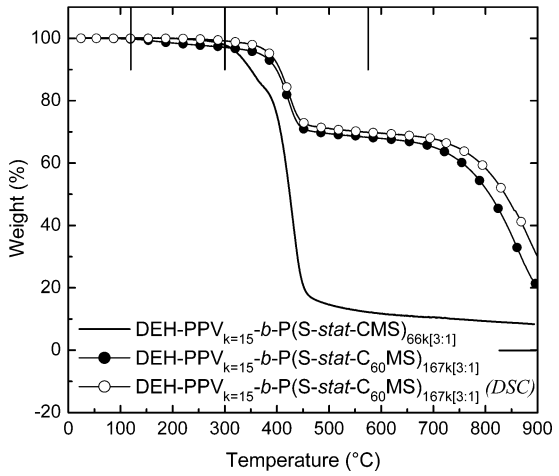

Figure 3. TGA traces of diblock copolymers before and after a DSC scan recorded under N_2 with a heating rate 10 °C/min.

synthesis. On the basis of our observations and the above-mentioned solubility problems (also observed by others), one could conclude that the azide intermediate route is not yet a versatile method to functionalize polymers with C_{60}.

Solid-State Properties of Diblock Copolymers Films. Control over the structure and morphology in the solid state of D−A diblock copolymers is important for the optoelectronic properties of photovoltaic devices based on these materials. Bässler proposed that charge transport in disordered organic materials proceeds mainly by means of hopping across the medium at three levels: intrachain, interchain, and interparticle (across grain boundaries).[41] Factors determining intra- and interchain transport are the conjugation length and structural order, respectively. Side chains attached to the polymer backbone have a contradictory effect on the transport properties at microscopic level. They may introduce torsions along the chain, decreasing thereby the conjugation length[42] or, as insulating side chains will, increase the hopping distance between neighboring chains. On the other hand, the hopping rate increases when the side chains enhance the ordering of polymer segments in the solid state. For example, highly regioregular polymers have an enhanced on-chain energetic order and charge delocalization.[43] Moreover, long side chains may have their own crystallization and melt behavior and can induce liquid crystallinity (LC) in rigid-rod-like macromolecules such as PPV.[44] PPV derivatives and rod−coil diblock copolymers have shown to possess a rich phase behavior.[45] Oligophenylenevinylenes with alkoxy side chains, so-called "hairy-rod" molecules, are extensively studied because of their reversible LC transitions.[46] This crystallization can lead to dramatic changes in the optical and electronic properties of a material.[47] The alignment of the backbones (with a π-stacking arrangement and side chains acting as spacers) may for example promote the interchain and intersegment electronic interactions. This increased amount of electronic overlap between segments and reduced structural heterogeneity is expected to enhance the charge transport.

LC behavior appears in a restricted temperature range between the crystalline phase and the isotropic melt. Having this, so-called, thermotropic LC behavior in the active layer of a PV device will introduce a temperature-dependent operation mode making the study of thermotropic transitions in thin films important. Moreover, the thermal stability of the conjugated polymer itself is important. In this section we report the thermal transitions of the homopolymers DEH−PPV$_{k=15,21}$ and DOO−PPV$_{k=7}$ in the solid state and compare them with those of the diblock copolymers. The homopolymers are the same as used for the synthesis of the corresponding diblock copolymers. The thermal properties are studied by DSC, TGA, and optical microscopy. DSC was used to determine the thermotropic transition temperatures like T_g, side-chain melting temperature (T_s), and the liquid-crystal-to-isotropic transition temperature (T_{LC-I}). The LC structure of polymer films was elucidated by optical microscopy using crossed polarizers.

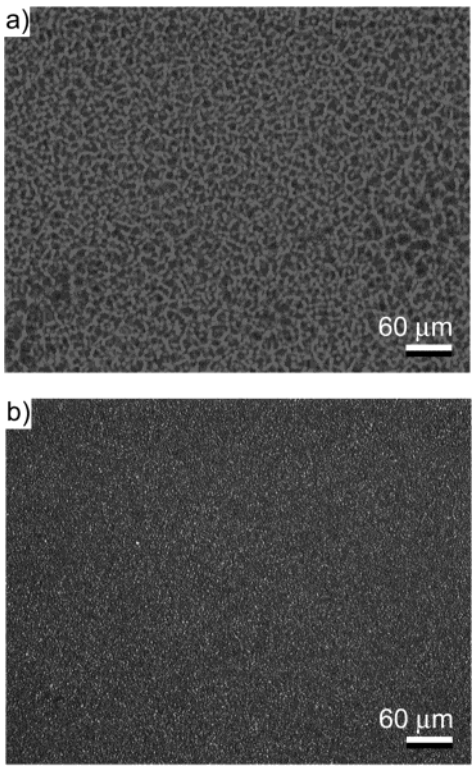

Figure 4. Optical micrographs at RT of the as-cast film (a) of DOO−PPV$_{k=7}$ and (b) using crossed polarizers for the film that was cooled from the isotropic melt to 90 °C.

DOO−PPV-Based Diblock (Co)polymers. The synthesis of DOO−PPV and its block copolymers is described in refs 25 and 31 and in the Experimental Section. The DSC analysis of DOO−PPV reveals the existence of thermotropic transitions at 55 and 185 °C, of which the lower transition temperature is attributed to melting of the octyloxy side chains (T_s) and the higher one to the isotropic transition temperature (T_{LC-I}). A 1 wt % solution of DOO−PPV in 1,2-dichlorobenzene (or chloroform) was cast onto a glass slide, and the film was investigated with optical microscopy. Figure 4a shows the rough texture of the as-cast film. It reveals reddish elongated domains that are randomly distributed in the film (displayed as gray areas in Figure 4a). Crossed polarizers were used to determine whether the film exhibits highly ordered crystalline domains. The absence of any birefringence in the as-cast film shows that it does not reveal any highly ordered crystalline domains.

A reddish grainy texture (or polydomain texture) is observed upon cooling from the isotropic melt at 250 to 90 °C (gray areas in Figure 4b). Such a birefringence

Table 3. Transition Temperatures of DOO−PPV and DEH−PPV-Based Diblock (Co)polymers and Their Corresponding Homopolymers

	T_g (°C)	T_s (°C)	T_{LC-I} (°C)[a]	T_{dec} (°C)[b]
DOO−$PPV_{k=7}$		55	185	380
DOO−$PPV_{k=9}$-*b*-PS_{22K}	95	60	160	370
DOO−$PPV_{k=9}$-*b*-$P4VP_{12.1K}$	150	70	190[c]	330
DOO−$PPV_{k=9}$-*b*-$PBA_{5.8K}$	−45	50	180	340
DOO−$PPV_{k=7}$-*b*-P(S-*stat*-CMS)$_{9K[1.5:1]}$	95	60	160	335
DOO−$PPV_{k=7}$-*b*-P(S-*stat*-C_{60}MS)$_{19K[1.5:1]}$	110	65	160	300
P(S-*stat*-CMS)$_{21K[2:1]}$	90			320
DEH−$PPV_{k=15}$		55/75	200	360
DEH−$PPV_{k=15}$-*b*-P(S-*stat*-CMS)$_{66K[3:1]}$	100	85	210	325
DEH−$PPV_{k=15}$-*b*-P(S-*stat*-N_3MS)$_{66K[3:1]}$	100	85	n.d.[d]	260
DEH−$PPV_{k=21}$		80	200	n.d.
DEH−$PPV_{k=21}$-*b*-P(S-*stat*-CMS)$_{14K[2.1:1]}$	85	90	210	n.d.
DEH−PPV^{50}		110	285	390

[a] In combination with optical microscopy. [b] Given for 5 wt % loss during TGA. [c] Determined by optical microscopy. [d] n.d. = not determined.

texture is often observed near the isotropic−nematic transition for polydisperse and high-molecular-weight specimens in thick films. The fine grains are believed to correspond to regions of uniform orientation interconnected by disclinations within nematic structures.[48] Hence, all diblock copolymers described below based on this symmetrically substituted DOO−PPV moiety have a rodlike diblock that exhibits liquid crystallinity. This does not imply a priori that all diblock copolymers based on this PPV block will also exhibit the same thermotropic behavior.

The thermotropic transitions of the DOO−PPV diblock (co)polymers obtained by a combination of DSC and optical microscopy as well as the decomposition temperature (T_{dec}) determined by TGA are given in Table 3. Although the T_g depends slightly on the molecular weight of the second coillike block, they represent typical T_g's (within a margin of ±5 °C) for the (di)block polymers. T_g's of the corresponding homopolymers (PS, 110 °C; PBA, −60 °C; P4VP, 145 °C)[49] differ up to 15 °C. The variation is attributed to the local order and the low molecular weight of the diblock polymers. The statistical copolymer P(S-*stat*-CMS)$_{21K[2:1]}$ exhibits a lower T_g compared to its corresponding diblock copolymer. Upon functionalization of DOO−PPV-*b*-P(S-*stat*-CMS) with C_{60} the polymer chain becomes stiffer, and consequently, its T_g increases from 95 to 110 °C. The T_s is only observed in the first heating scan of the DSC analysis, implying that the crystallization of the octyloxy side chains is a slow process and depends on the (thermal) history of the sample. The melting temperature of the side chains also depends on the T_g of the second block. With increasing T_g of this coillike block the T_s shifts toward higher temperatures due to a relative higher stiffness of their local environment. Illustrative of this phenomenon is DOO−PPV-*b*-PBA with a T_g of −45 °C. Its very low T_g results in soft and flexible microdomains that allows the octyloxy side chains to melt at lower temperatures. Vice versa, a PBA homopolymer has a T_g of −60 °C, and the increased T_g of −45 °C for the diblock polymer suggests the presence of PPV blocks between the PBA domains. All other diblock (co)polymers exhibit T_g's above the side-chain

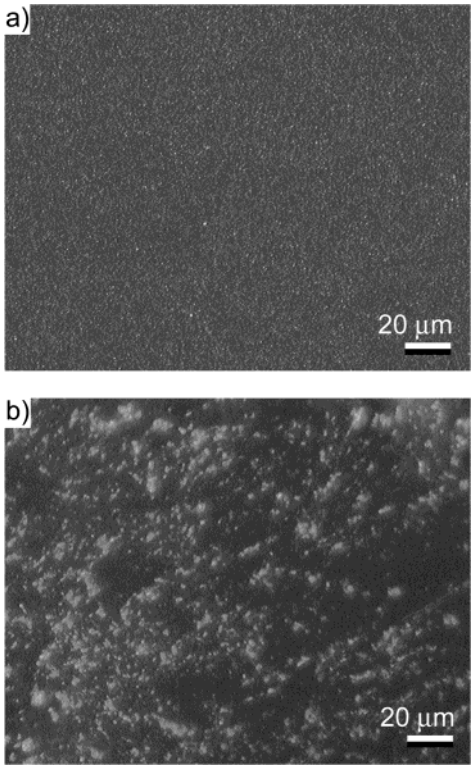

Figure 5. Optical micrographs at RT using crossed polarizers of (a) DOO−$PPV_{k=9}$-*b*-$P4VP_{12.1K}$ as-cast and (b) after cooling from the melt and annealing for 1 h at 150 °C.

melting temperature, resulting in higher values of T_s compared to the that of DOO−PPV homopolymer. This is attributed to the glassy environment induced by the coillike block below its T_g. For the polydisperse DOO−PPV one does not observe a clear isotropic transition temperature (T_{LC-I}) of the backbone with DSC, but merely a continuous increase of the endothermic heat flow above a certain temperature. Hence, the onset of the increased heat flow is taken as the T_{LC-I} of the DOO−PPV backbone. The DOO−PPV-*b*-P4VP showed a continuous increase of the heat flow directly above its glass transition. The broad T_g of the P4VP block around 150 °C is close to the melting temperature of the PPV backbone and masks the onset of the T_{LC-I}. This latter transition was therefore determined with optical microscopy, resulting in a slightly higher T_{LC-I} compared to a DSC analysis. In general, the series of DOO−PPV-based diblock copolymers reveal distinct transition temperatures for both blocks, suggesting that microphases are involved. For a homogeneous mixture only one transition from the glassy state to the liquid state would have been observed.

Drop-casting a 1 wt % solution of DOO−PPV-*b*-PS, DOO−PPV-*b*-P4VP, or DOO−PPV-*b*-PBA in chloroform onto glass slides and subsequent slow evaporation of the solvent resulted in thick films that showed birefringence when imaged by optical microscopy (Figure 5a). All diblock polymers gave rise to similar grainy textures as their corresponding homopolymer DOO−PPV (Figure 4b). Upon heating to the isotropic melt the DOO−PPV-*b*-PBA started to dewet the surface at 180 °C, which resulted in small cracks in the film. DOO−PPV-*b*-PS and DOO−PPV-*b*-P4VP liquefied above their T_{LC-I}, but dewetting was not observed. The LC phases emerged at temperatures that were 20−30 °C below the melting temperatures of the DOO−PPV backbone. In Figure 5b,

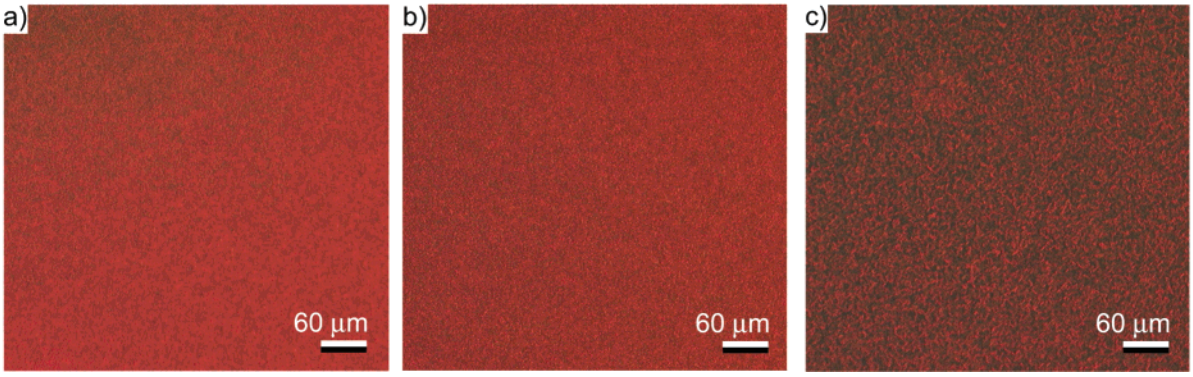

Figure 6. Optical micrographs at RT using crossed polarizers of (a) DEH−PPV$_{k=15}$, (b) DEH−PPV$_{k=21}$, and (c) DEH−PPV$_{k=21}$-*b*-P(S-*stat*-CMS)$_{14K[2.1:1]}$.

an optical micrograph of DOO−PPV-*b*-P4VP displays the typical crystalline texture at RT that was obtained by cooling from the melt down to 150 °C and subsequent annealing at 150 °C for 1 h prior to the cooling to RT. Generally, this cooling from the melt gave rise to larger crystalline domains compared to the as-cast films (Figure 5, b vs a, respectively). The drop-casting of more diluted diblock copolymer solutions (0.1 wt %) followed by rapid evaporation of the solvent did not give rise to birefringence or crystalline domains. This is attributed to a fast solidification process rendering a long-range order in the polymer films. The microphases can be ordered locally on a length scale of several tens of nanometers (see AFM images in ref 24). On a large scale, however, the films appear to be isotropic due to the overall random orientation of small domains. Because the resolution of optical microscopy is limited to the wavelength of light, one cannot reveal the local order in these films using this technique and has to utilize other techniques like AFM or TEM.[31]

DEH−PPV-Based Diblock Copolymers. The DEH−PPV homopolymers show a similar behavior as the DOO−PPV with the PPV backbone as the mesogenic group. The DEH−PPV$_{k=15}$ shows two transitions at low temperatures (55 and 75 °C, Table 3), which are both attributed to melting of the side chains. For DEH−PPV$_{k=21}$ only a single transition is found, which covers the same temperature range. Since we observed several crystalline-like textures in films of this polymer (optical microscopy is described below), it is reasonable to assume that this single and broad transition comprises to the two transition temperatures found for the DEH−PPV$_{k=15}$ homopolymer. Clear isotropic transition temperatures of the DEH−PPV (T_{LC-I}) are not found with DSC. The observed continuous increase of heat flow may be due to crystallites that differ in size and perfection. To circumvent these difficulties, we used optical microscopy to determine the T_{LC-I} as the onset of the fast disappearance of birefringence.

The amorphous P(S-*stat*-CMS) block in the DEH−PPV diblock copolymers gives rise to a clear T_g transition. In line with the theory this T_g increases (from 85 to 90 or 100 °C) for increasing P(S-*stat*-CMS) block lengths (14, 21, and 66 kg/mol, respectively). However, the T_s is now more difficult to elucidate because it coincides with the T_g of the P(S-*stat*-CMS) block. For both chain extended DEH−PPV$_{k=15,21}$ polymers the T_s increases with 10 °C. The mobility of segments at specific temperatures seems to be lower due to the glassy environment introduced by the P(S-*stat*-CMS). Furthermore, the T_s for the DEH−PPV-*b*-P(S-*stat*-CMS) diblock copolymer is only found during the first heating scan. After crystallization upon cooling, the corresponding endothermic peak in the following heating scan is absent probably due to a smaller volume fraction of crystalline material.

Optical microscopy reveals the presence of birefringent textures in thick films of DEH−PPV and DEH−PPV-*b*-P(S-*stat*-CMS). The films were obtained after drop-casting a 1 wt % solution in chlorobenzene onto glass slides and a subsequent slow evaporation of the solvent. The as-cast films appeared to be highly birefringent when examined under crossed polarizers. They exhibit reddish needlelike domains that are isotropically distributed in the film (Figure 6). The amorphous domains (black) as well as the crystalline domains increase in size with increasing DEH−PPV block lengths (Figure 6, a and b, respectively). A significant increase in size of both domains is observed in films of DEH−PPV-*b*-P(S-*stat*-CMS) (Figure 6, b vs c). Apparently, this second coillike block enhances the mobility of the DEH−PPV, resulting in a facilitated crystallization from solution and larger domains. Heating of the films resulted in melting of the crystalline domains, but no reversible birefringence was observed after the subsequent cooling from the melt. This indicates that the crystallization of the bulk polymer is a slow process. No efforts have been made to (re)crystallize the polymer by means of annealing at temperatures just above the T_g or T_s as has been done for DOO−PPV-*b*-P4VP (Figure 5b). In addition to the randomly distributed needlelike domains, we find spherical aggregates often called spherulites.

The thermotropic transitions of the C_{60}-functionalized DEH−PPV diblock copolymers are not included in this study since they show exothermic reactions upon heating (i.e., extrusion of nitrogen, see discussion of Figure 3). The C_{60} incorporated in DOO−PPV-*b*-P(S-*stat*-CMS) did increase the chain stiffness and changed its thermotropic LC behavior. Similar results are expected for the DEH−PPV polymers, suggesting a temperature-dependent operation mode for optoelectronic devices based on these donor−acceptor diblock copolymers.

Conclusions

An improved synthesis of the NMRP macroinitiator based on PPV and TIPNO is presented, which is used for the preparation of donor−acceptor diblock copolymers. A "living" character of the NMRP polymerizations is observed for these PPV-based macroinitiators. The block lengths as well as the built-in ratio of the comonomers in the second P(S-*stat*-CMS) block can be con-

trolled during the course of the polymerization. The macroinitiator allows for the adjustment of the donor−acceptor ratio in the C_{60}-functionalized diblock copolymers. In addition, the method to introduce the C_{60} has been improved by circumventing the formation of radicals through the utilization of azide intermediates. Further improvement of this new approach is necessary to enhance the solubility of the donor−acceptor diblock copolymers. This could be achieved by means of a complete conversion of the azide intermediates.

The structure−property relationship of the (diblock co)polymers is investigated using the DOO−PPV and DEH−PPV homopolymers as reference compounds. They are both liquid-crystalline and exhibit thermotropic transitions at 55 and 185 °C for DOO−$PPV_{k=7}$ and 80 and 200 °C for DEH−$PPV_{k=21}$. The first transition is attributed to the melting of the side chains, and the second higher one is an isotropic transition. Consequently, the diblock copolymers possess complex and rich phase behavior due to the combination of a mesogenic rodlike block and the adjacent coillike block. An additional thermotropic transition was identified for the diblock copolymers that is attributed to the T_g of the polystyrene-like block.

We have shown that this approach of rational design and controlled synthesis is a systematic method to explore the correlation between (self-)organization of rod−coil diblock copolymers and the morphology of films thus produced (and ultimately the correlation between self-organization and the device performance).

Experimental Section

Measurements. ^{1}H NMR spectra were recorded on a Varian Gemini-300 spectrometer operating at 300 MHz in the Fourier transform mode. All measurements were performed at room temperature (RT) in chloroform-*d* ($CDCl_3$; internal lock on the ^{2}H signal). Absorbance spectra were recorded on a Perkin-Elmer Instruments Lambda 900 UV/vis/NIR spectrometer and normalized of clarity. Fluorescence spectra were recorded on a Perkin-Elmer luminescence spectrometer LS50-B using an excitation wavelength of 10 nm below the absorption maximum and a 2.5 nm bandwidth. The optical measurements were performed in Uvasol chloroform with quartz cuvettes (light path 10 mm) unless mentioned otherwise. Gel permeation chromatography (GPC) analyses were performed in THF (HPLC grade) with PL-gel mixed-C columns in a Waters Powerline setup (717^{plus} autosampler, 600 controller, and a 610 fluid unit), equipped with a Waters 996 photodiode array detector (on-line UV−vis measurements), a Wyatt Dawn DSP laser photometer (light scattering detector), and a 410 differential refractormeter. All solutions (∼1 mg/mL) were filtered over a polystyrene filter (0.45 μm) prior to a duplicate injection of 100 μL (flow 1 mL/min, run time 25 min, RT). The infrared spectra were recorded on a Mattson Instruments FT-IR spectrometer. Optical microscopy was performed on a Zeiss Axiophot microscope equipped with a high-resolution CCD camera (Sony DKC 5000; connected to a frame grabber and a personal computer). Heating of the polymer films was performed in a Mettler FP82HT optical hot stage with a Mettler FP90 controller. Thermogravimetric analyses (TGA) were carried out using a Perkin-Elmer TGA7 (heating rate of 10 °C/min under a N_2 atmosphere). Differential scanning calorimetry (DSC) analyses were obtained with a Perkin-Elmer DSC-7 (calibrated with indium).

Materials. The syntheses of DOO−$PPV_{k=7}$ homopolymer, DOO−$PPV_{k=7}$-*b*-P(S-*stat*-CMS)$_{9k[1.5:1]}$, and DOO−$PPV_{k=7}$-*b*-P(S-*stat*-C_{60}MS)$_{19K[1.5:1]}$ diblock copolymers are described in ref 25, of DOO−$PPV_{k=9}$-TIPNO and DOO−$PPV_{k=9}$-*b*-$PBA_{5.8K}$ in ref 31, and of DOO−$PPV_{k=9}$-*b*-PS_{22K} in ref 24. Styrene (S) and 4-chloromethylstyrene (CMS) were distilled before use from CaH_2 under reduced pressure. Additional purification of CMS was necessary by means of filtration over basic aluminum oxide (90 Active Base, 0.063−0.200 mm). Anisole was distilled from Na, THF from Na/K alloy, CH_2Cl_2 from Ca, toluene from Na/benzophenone, and ether from KOH and $LiAlH_4$. DMF was stored on molecular sieve 4 Å, while all other solvents were used as received unless mentioned otherwise. All NMRPs were carried out under a N_2 atmosphere.

DOO−PPV_k-*b*-P4VP. The macroinitiator DOO−$PPV_{k=9}$−TIPNO (0.2 g, $M_{n,PPV} = 3.9 \times 10^3$ g/mol), freshly distilled 4-vinylpyridine (4VP, 10 g, 95 mmol), anisole (10 mL), acetic anhydride (Ac_2O, 0.2 g, 2 mmol), and 2,2,5-trimethyl-4-phenyl-3-azahexane-3-oxy (TIPNO free radical, 2 mg, 0.009 mmol) were degassed by freeze−pump−thaw cycles (3×), flushed with N_2, and polymerized at 110 °C. Samples were taken after 4 and 8 h and precipitated in hexane (1 L). The polymer was precipitated from $CHCl_3$ into hexane (1 L). Yields: 189 mg (4 h) and 373 mg (8 h). Molecular weight $M_n = 7.1$ and 16.0×10^3 g/mol, respectively, determined by ^{1}H NMR. ^{1}H NMR: $\delta = 8.0-8.6$ (br d, $C^{ar}H$), 7.4 (br s, $C^{olef}H$), 7.11 (br s, $C^{ar}H$), 6.2−6.6 (br d, $C^{ar}H$), 4.0 (br s, OCH_2), 2.2 (br s, $C^{ar}H_3$), 1.3−1.8 (m, CH, CH_2), 0.8 (s, CH_3).

2,5-Di(2′-ethyl)hexyloxy-4-methylbenzaldehyde (1). The monomer is prepared via the etherification of methylhydroquinon with (2′-ethyl)hexyl bromide[51] (purified by means of Kugelrohr at 100 °C/ 0.01 mbar; yield 62%; yellow oil), followed by a selective Rieche-Gross formylation with dichloro(methoxy)-methane.[52] After purification by means of Kugelrohr (117−122 °C/ 0.7 mbar), monomer **1** was obtained as yellow oil (78% yield). ^{1}H NMR: $\delta = 10.38$ (s, 1H, CHO), 7.17 (s, 1H, $C^{ar}H$), 6.75 (s, 1H, $C^{ar}H$), 3.7−3.9 (dd, 4H, OCH_2), 2.22−2.42 (br s, 3H, $C^{ar}CH$), 1.7 (m, 4H, CH_2), 1.2−1.4 (br m, 18H, CH, CH_2), 0.9 (m, 12H, CH_3).

DEH−PPV_k. The synthesis of DEH−PPV was accomplished by the Siegrist polycondensation (originally described in ref 30) of compound **1**. The average degree of polymerization (i.e., number of repeat units *k*) of the DEH−PPV is determined with ^{1}H NMR spectroscopy using the ratio of integrals of the OCH_2 groups and the terminal CH_3 group. For a DEH−PPV polymer prepared at 80 °C in 3 h, a *k* of 21 units is calculated by this method. This so-called DEH−$PPV_{k=21}$ has a polydispersity (PD) of 1.23 (determined by means of GPC vs polystyrene standards) and a $M_n = 7.9 \times 10^3$ g/mol. By *only* changing the temperature to 50 °C, the DEH−$PPV_{k=15}$ was synthesized in 3 h with PD = 1.16 and $M_n = 5.6 \times 10^3$ g/mol. Representative ^{1}H NMR of DEH−$PPV_{k=21}$: $\delta = 10.41$ (s, CHO/end group), 7.49 (br s, $C^{olef}H$), 6.67−7.16 (br s, $C^{ar}H$), 3.91 (br m, OCH_2), 2.20−2.34 (br s, CH_3/end group), 1.71−1.85 (m, CH_2), 1.14−1.68 (m, CH, CH_2), 0.8−1.0 (m, CH_3).

DEH−PPV_k−TIPNO. The $Br_2Mg-O(C_2H_5)_2$ is prepared prior to the synthesis from a stirred mixture under a dry N_2 atmosphere of Mg turnings (0.17 g, 7.0 mmol) and ether (5 mL). Via a syringe, 1,2-dibromoethane (0.55 mL, 6.38 mmol) was slowly added, and the mixture was stirred at RT for 30 min. From the resulting two-phase mixture, a quarter of lower gray layer was used in the synthesis of DEH−$PPV_{k=21}$−TIPNO. For this, 2,2,5-trimethyl-3-[1-(4-bromophenyl)ethoxy]-4-phenyl-3-azahexane[53] **(2)** (0.62 g, 1.5 mmol) was dissolved in ether (10 mL) and cooled to −80 °C (cryostat). After the addition of *tert*-butyllithium (1.5 M in pentane, 2 mL, 3 mmol), the solution was stirred for 30 min at −80 °C. During this time, the originally colorless solution turned via yellow to orange. After adding the freshly prepared $Br_2Mg-O(C_2H_5)_2$ (∼1.75 mmol), a cloudy, white suspension, containing compound **3**, was obtained. This was allowed to warm to RT. After 30 min, the color turned to yellow when the stirred solution was immersed in a thermostated oil bath kept at 35 °C. A solution of DEH−$PPV_{k=21}$ (1.4 g, 0.18 mmol) in ether (40 mL) was added via a syringe and stirred for 16 h at 35 °C. The mixture was quenched in water (150 mL) that contained HCl (37%, 3 mL) and stirred for 30 min at RT. After this period, the mixture was extracted with ether (200 mL), the organic layer was washed with water (2 × 300 mL) and with saturated $NaHCO_3$ (1 × 200 mL), dried over Na_2SO_4, and filtered, and the solvent was removed under a reduced pressure at RT. The red solid was dissolved in $CHCl_3$ (10 mL) precipitated twice in cold

methanol (400 mL, ca. −30 °C), washed with ethanol until a colorless filtrate was obtained (to remove excess of **3**), and dried under reduced pressure (RT, 16 h). Yield: 1.08 g (76%) of red powder. Using the same conditions, the reaction has also been performed with DEH−$PPV_{k=15}$, resulting in 0.39 g (68%) of DEH−$PPV_{k=15}$−TIPNO. ^{1}H NMR: δ = 7.49 (br s, $C^{olef}H$), 6.67−7.16 (br s, $C^{ar}H$), 5.90 (br m, C*H*OH), 4.85 (br m, OC*H*CH_3), 3.91 (br m, OCH_2), 3.37 (d, NC*H*CH), 2.96 (br s, CHO*H*), 2.20−2.34 (s, CH_3/end group), 1.71−1.85 (m, CH_2), 1.14−1.68 (m, C*H*, CH_2), 0.8−1.0 (m, CH_3), 0.50 (d, CH(CH_3)$_2$ TIPNO).

DEH−PPV_k-*b*-P(S-*stat*-CMS)$_{p[n:m]}$. The macroinitiator DEH−PPV−TIPNO was chain extended with a statistical copolymer by mixing the appropriate amounts of styrene and 4-chloromethylstyrene. The nomenclature used for the second block is as follows: *p* is the molecular weight ($M_n \times 10^3$ g/mol) of the statistical copolymer with a built-in S to CMS ratio indicated by *n* and *m*, respectively. The molar ratio of macroinitiator to comonomer was in all cases 1:1300. Relative to the amount of DEH−PPV−TIPNO, 4 equiv of Ac_2O and 0.1 equiv of TIPNO free radical (6 mg/mL in anisole) were added. Equal weights of anisole to comonomer were used (optional). The resulting solution was mixed and degassed by freeze−pump−thaw cycles (3×), flushed with dry N_2, and subsequently immersed in a thermostated oil bath at 125 °C. The mixture was cooled to RT after the desired polymerization time. The polymer was precipitated in large excess of cold methanol (ca. −30 °C), filtered, and washed until a colorless filtrate was obtained. After redissolving in $CHCl_3$ (few milliliters), the polymer was again precipitated into cold methanol, filtered, and washed. After drying under reduced pressure (60 °C, 16 h), an orange powder was obtained.

DEH−$PPV_{k=15}$-*b*-P(S-*stat*-CMS)$_{65K[3:1]}$. DEH−$PPV_{k=15}$−TIPNO (0.14 g, 0.025 mmol), S (2.84 g, 27.3 mmol), CMS (1.04 g, 6.81 mmol), Ac_2O (10 μL, 0.11 mmol), TIPNO (0.62 mg, 0.003 mmol); bulk polymerization with samples taken after time intervals; yields: 5 mg (40 min, PD = 1.2), 0.14 g (100 min, PD = 1.7), 0.13 g (120 min, PD = 1.8), and 0.58 g (140 min, PD = 2.2). The last sample has been functionalized with C_{60}.

DEH−$PPV_{k=21}$-*b*-P(S-*stat*-CMS)$_{14K[2.1:1]}$. DEH−$PPV_{k=21}$−TIPNO (0.41 g, 0.05 mmol), S (5.47 g, 52.4 mmol), CMS (2.49 g, 16.3 mmol), Ac_2O (20 μL, 0.21 mmol), TIPNO (1.1 mg, 0.005 mmol), anisole (7.96 g, 73.6 mmol); yield: 0.86 g (conversion of 13% in 50 min, PD = 1.5).

DEH−$PPV_{k=21}$-*b*-P(S-*stat*-CMS)$_{31K[2.6:1]}$. DEH−$PPV_{k=21}$−TIPNO (0.39 g, 0.05 mmol), S (5.43 g, 52.1 mmol), CMS (2.24 g, 14.7 mmol), Ac_2O (20 μL, 0.21 mmol), TIPNO (1.1 mg, 0.005 mmol), anisole (7.98 g, 74.2 mmol); yield: 1.45 g (conversion of 23% in 80 min, PD = 1.8). Representative ^{1}H NMR of DEH−$PPV_{k=21}$-*b*-P(S-*stat*-CMS)$_{14K[2.1:1]}$: δ = 7.49 (br s, $C^{olef}H$), 6.66−7.01 (br m, $C^{ar}H$), 4.46 (br s, CH_2Cl), 3.91 (br m, OCH_2), 2.20−2.34 (br s, CH_3/end group), 1.04−1.9 (m, C*H*, CH_2), 0.8 (br m, CH_3), 0.45 (br s, CH(CH_3)$_2$ TIPNO).

DEH−PPV_k-*b*-P(S-*stat*-N_3MS)$_{p[n:m]}$. The corresponding diblock copolymers and NaN_3 (20 equiv relative to the built-in amount of CMS comonomer) were mixed in DMF (100 mL). After stirring for 16 h at 130 °C (no N_2 atmosphere), the reaction mixture was poured out in water (300 mL) containing $CHCl_3$ (50 mL). After stirring for 15 min, the mixture was extracted with $CHCl_3$ (2 × 50 mL). Water (300 mL) was then added to the combined organic layers. After stirring for 15 min, the water layer was extracted with $CHCl_3$ (200 mL). Each portion of the combined organic layers (200 mL) was separately washed with water (400 mL). The organic layers were dried over Na_2SO_4 and filtered, and the solvent was removed. Dissolved in $CHCl_3$ (10 mL), the polymer was precipitated twice into cold methanol (400 mL, ca. −30 °C) and washed until a colorless filtrate was obtained. The product was dried under reduced pressure (30 °C, 16 h), resulting in an orange powder.

DEH−$PPV_{k=15}$-*b*-P(S-*stat*-N_3MS)$_{67K[3:1]}$. DEH−$PPV_{k=21}$-*b*-P(S-*stat*-CMS)$_{66K[3:1]}$ (0.32 g, 0.004 mmol), NaN_3 (0.83 g, 12.8 mmol); yield: 0.27 g (85%).

DEH−$PPV_{k=21}$-*b*-P(S-*stat*-N_3MS)$_{14K[2.1:1]}$. DEH−$PPV_{k=21}$-*b*-P(S-*stat*-CMS)$_{14K[2.1:1]}$ (0.83 g, 12.8 mmol), NaN_3 (1.47 g, 22.6 mmol); yield: 0.50 g (76%).

DEH−$PPV_{k=21}$-*b*-P(S-*stat*-N_3MS)$_{31K[2.6:1]}$. DEH−$PPV_{k=21}$-*b*-P(S-*stat*-CMS)$_{31K[2.6:1]}$ (1.0 g, 0.026 mmol), NaN_3 (2.41 g, 37.1 mmol); yield: 0.87 g (85%). Representative ^{1}H NMR of DEH−$PPV_{k=21}$-*b*-P(S-*stat*-N_3MS)$_{14K[2.1:1]}$: δ = 10.41 (s, C*H*O/end group), 7.49 (br s, $C^{olef}H$), 6.66−7.01 (br m, $C^{ar}H$), 4.17 (br s, CH_2N_3), 3.91 (br m, OCH_2), 2.20−2.34 (br s, CH_3/end group), 1.04−1.9 (m, C*H*, CH_2), 0.8 (br m, CH_3). Representative IR (FT-IR) of DEH−$PPV_{k=15}$-*b*-P(S-*stat*-N_3MS)$_{67K[3:1]}$: 3026 (w, $-C_{aryl}-H$), 2923 and 2854 (s, CH_3 and CH_2), 2094 (vs, CN_3), 1601 (s, $-C{=}C-_{aryl}$), 1493 and 1453 (s, $-C_6H_5$, in plane), 1264 (s, $C_{aryl}-OR$), 1199 and 1029 (s, $-C_{aryl}-H$ = , out-of-plane), 817 and 756 (w and vs, $-C_{aryl}-H$ = , in-plane) cm^{-1}.

DEH−PPV_k-*b*-P(S-*stat*-C_{60}MS)$_{p[n:m]}$. The corresponding (di)block copolymers and C_{60} (2 equiv relative to the amount of N_3MS comonomer) were dissolved in chlorobenzene and degassed by bubbling dry N_2 through the solution for 15 min. The mixture was stirred at 60 °C for 20 h using a thermostated oil bath. Subsequently, it was refluxed for 1 h at 130 °C (no N_2 atmosphere). After cooling to RT, saturated NaCl (10 mL) was added, and the mixture was vigorously stirred for 1 h as an attempt to remove unreacted azide groups. The organic layer was washed with water (4 × 500 mL) and dried over Na_2SO_4, and the solvent was almost completely removed. The residue was diluted with THF (500 mL), filtered, and washed until a colorless filtrate, and the THF was removed under reduced pressure. After repeating this latter step, the polymer was precipitated in methanol (200 mL), filtered, and taken up in chlorobenzene (10 mL). This latter precipitation and filtration were repeated, and the product was either dried under reduced pressure (70 °C, 16 h) or stored in chlorobenzene (10 mL).

DEH−$PPV_{k=15}$-*b*-P(S-*stat*-C_{60}MS)$_{167K[3:1]}$. DEH−$PPV_{k=21}$-*b*-P(S-*stat*-N_3MS)$_{67K[3:1]}$ (0.24 g, 0.0033 mmol), C_{60} (0.68 g, 0.94 mmol); yield: 0.24 g (42%) of reddish-brown powder (poorly soluble in organic solvents).

DEH−$PPV_{k=21}$-*b*-P(S-*stat*-C_{60}MS)$_{41K[2.1:1]}$. DEH−$PPV_{k=21}$-*b*-P(S-*stat*-N_3MS)$_{14K[2.1:1]}$ (0.40 g, 0.018 mmol), C_{60} (1.0 g, 1.4 mmol); yield: 10−15 mL (34 mg/g chlorobenzene) of reddish-brown solution.

P(S-*stat*-C_{60}MS)$_{63K[2:1]}$. This reference compound was prepared from P(S-*stat*-N_3MS)$_{21K[2:1]}$ (36 mg, 0.0017 mmol) and 1 equiv (!) of C_{60} (66 mg, 0.092 mmol); yield: 27 mg (26%) of brown powder (poorly soluble in organic solvents). Representative ^{1}H NMR of DEH−$PPV_{k=21}$-*b*-P(S-*stat*-C_{60}MS)$_{41K[2.1:1]}$: δ = 10.41 (s, C*H*O/end group), 6.25−7.48 (br m, $C^{ar}H$, $C^{olef}H$), 3.88 (br m, OCH_2), 2.20−2.34 (s, CH_3/end group), 1.04−1.9 (m, C*H*, CH_2), 0.8 (br m, CH_3).

P(S-*stat*-CMS)$_{21K[2:1]}$. Styrene (S, 10.89 g, 104.6 mmol) and 4-chloromethylstyrene (CMS, 8.00 g, 52.4 mmol) were mixed with an alkoxyamine based on TIPNO (i.e., 2,2,3-trimethyl-3-(1-phenylethoxy)-4-phenyl-3-azahexane; synthesized according to ref 53; 0.20 g, 0.61 mmol). After addition of Ac_2O (0.21 g, 2.06 mmol), the mixture was degassed by freeze−pump−thaw cycles (3×) and flushed with dry N_2. Immersed in a thermostated oil bath it was kept at 125 °C for 5 h. Samples were taken (after 80, 110, 160—when the reaction mixture solidified—, 180, 230, and 270 min), which were diluted with $CHCl_3$, precipitated twice in methanol, filtered, and washed. The products were dried under reduced pressure (60 °C, 16 h). Yields of white powder: 0.48 g (from 1.19 g; 80 min, PD = 1.1), 0.34 g (from 0.56 g; 110 min, PD = 1.1), 64 mg (from 0.13 g; 160 min, PD = 1.2), 0.66 g (from 0.74 g; 180 min, PD = 1.2), 0.83 g (from 0.90 g; 230 min, PD = 1.2), 0.83 g (from 0.89 g; 270 min, PD = 1.2), and 13.7 g (from 14 g; final product after 300 min). The sample taken at 110 min was used as reference compound in subsequent syntheses (azide preparation and C_{60} functionalization). Representative ^{1}H NMR (sample of 110 min): δ = 6.50−7.00 (br s, $C^{ar}H$), 4.33−4.47 (br d, CH_2Cl), 1.36−1.73 (br s, C*H*, CH_2), 0.16−0.48 (br s, CH(CH_3)$_2$ TIPNO).

P(S-*stat*-N_3MS)$_{21K[2:1]}$. The P(S-*stat*-CMS)$_{21K[2:1]}$ (0.3 g, 0.014 mmol) and NaN_3 (1.08 g, 16.6 mmol) were mixed in DMF (50 mL). After stirring for 16 h at 130 °C (no N_2 atmosphere), the mixture was poured out in water (450 mL) containing $CHCl_3$ (50 mL). After stirring for 15 min, the mixture was extracted

with $CHCl_3$ (3 × 250 mL). The combined organic layers were concentrated and, after dissolving it in DMF (10 mL), precipitated into water (2 × 150 mL) and filtered. The product was dried under reduced pressure (60 °C, 16 h) and used as reference compound in the C_{60} functionalization (azide intermediate route to DEH−PPV-*b*-P(S-*stat*-C_{60}MS)). Yield: 0.21 g (67%) of white powder. ^{1}H NMR: $\delta = 6.50$, 7.00 (br s, $C^{ar}H$), 3.92−4.26 (br m, CH_2N_3), 1.36−1.73 (br s, C*H*, CH_2).

Acknowledgment. The following people are acknowledged for their contribution to the work described: P. F. van Hutten, G. O. R. Alberda van Ekenstein, E. J. Vorenkamp, C. Melzer, J. Wildeman, V. V. Krasnikov, S. Polychronopoulou, and H. Nijland. We thank FOM, NWO-CW, and the EU (TMR scholarship for U.S.) for their financial support.

Supporting Information Available: Additional FT-IR and UV−vis spectra of DEH−PPV-*b*-P(S-*stat*-CMS), DEH−PPV-*b*-P(S-*stat*-N_3MS), DEH−PPV-*b*-P(S-*stat*-C_{60}MS), and DEH−PPV−TIPNO (UV−vis only) visualize the functionalization with the azide group and incorporation of C_{60}. This material is available free of charge via the Internet at http://pubs.acs.org.

References and Notes

(1) Gilch, H. G.; Wheelwright, W. L. *J. Polym. Sci., Part A1* **1966**, *4*, 1337−1349.
(2) (a) Wessling, R. A.; Zimmerman, R. G. U.S. Patents 3,401,-152, 1968, and *Chem. Abstr.* **1968**, *69*, 87735q. (b) Wessling, R. A. *J. Polym. Sci., Polym. Symp.* **1985**, *72*, 55−66.
(3) (a) Heck, R. F. *Pure Appl. Chem.* **1978**, *50*, 691−701. (b) Bao, Z.; Chen, Y.; Cai, R.; Yu, L. *Macromolecules* **1993**, *26*, 5281−5286. (c) Hilberer, A.; Brouwer, H.-J.; van der Scheer, B.-J.; Wildeman, J.; Hadziioannou, G. *Macromolecules* **1995**, *28*, 4525−4529.
(4) Kossmehl, G.; Samandari, M. *Makromol. Chem.* **1985**, *186*, 1565−1574.
(5) Boutagy, J.; Thomas, R. *Chem. Rev.* **1974**, *74*, 87−99.
(6) Rehahn, M.; Schlüter, A. D. *Makromol. Chem., Rapid Commun.* **1990**, *11*, 375−379.
(7) Segura, J. L. *Acta Polym.* **1998**, *49*, 319−344.
(8) (a) Hempenius, M. A.; Langeveld-Voss, B. M. W.; van Haare, J. A. E. H.; Janssen, R. A. J.; Sheiko, S. S.; Spatz, J. P.; Möller, M.; Meijer, E. W. *J. Am. Chem. Soc.* **1998**, *120*, 2798−2804. (b) Li, W.; Maddux, T.; Yu, L. *Macromolecules* **1996**, *29*, 7329−7334.
(9) Li, W.; Wang, H.; Yu, L.; Morkved, T. L.; Jaeger, H. M. *Macromolecules* **1999**, *32*, 3034−3044.
(10) Wang, H.; Wang, H. H.; Urban, V. S.; Littrell, K. C.; Thiyagarajan, P.; Yu, L. *J. Am. Chem. Soc.* **2000**, *122*, 6855−6861.
(11) (a) Zhong, X. F.; François, B. *Synth. Met.* **1989**, *29*, E35−E40. (b) Zhong, X. F.; François, B. *Makromol. Chem.* **1991**, *192*, 2277−2291. (c) François, B.; Olinga, T. *Synth. Met.* **1993**, *55*−*57*, 3489−3494. (d) François, B.; Widawski, G.; Rawiso, M.; Cesar, B. *Synth. Met.* **1995**, *69*, 463−466. (e) Osaheni, J. A.; Jenekhe, S. A. *J. Am. Chem. Soc.* **1995**, *117*, 7389−7398. (f) Jenekhe, S. A.; Chen, X. L. *Science* **1998**, *279*, 1903−1907. (g) Francke, V.; Räder, H. J.; Geerts, Y.; Müllen, K. *Macromol. Rapid Commun.* **1998,** *19*, 275−281. (h) Marsitzky, D.; Brand, T.; Geerts, Y.; Klapper, M.; Müllen, K. *Macromol. Rapid Commun.* **1998**, *19*, 385−389. (i) Bianchi, C.; Cecchetto, E.; François, B. *Synth. Met.* **1999**, *102*, 916−917. (j) Mignard, E.; Tachon, C.; François, B. *Synth. Met.* **1999**, *102*, 1246−1247. (k) Klaerner, G.; Trollsås, M.; Heise, A.; Husemann, M.; Atthoff, B.; Hawker, C. J.; Hedrick, J. L.; Miller, R. D. *Macromolecules* **1999**, *32*, 8227−8229. (l) Leclère, P.; Calderone, A.; Marsitzky, D.; Francke, V.; Geerts, Y.; Müllen, K.; Brédas, J. L.; Lazzaroni, R. *Adv. Mater.* **2000**, *12*, 1042−1046. (m) Chen, X. L.; Jenekhe, S. A. *Macromolecules* **2000**, *33*, 4610−4612.
(12) (a) Halperin, A. *Macromolecules* **1990**, *23*, 2724−2731. (b) Hołyst, R.; Oswald, P. *Macromol. Theory Simul.* **2001**, *10*, 1−16. (c) Hołyst, R.; Schick, M. *J. Chem. Phys.* **1992**, *96*, 730−739. (d) Matsen, M. W.; Barrett, C. *J. Chem. Phys.* **1998**, *109*, 4108−4118.
(13) (a) Schulze, U.; Reichelt, N.; Schmidt, H.-W. *Macromol. Symp.* **1997**, *117*, 131−140. (b) Leclère, P.; Parente, V.; Brédas, J. L.; François, B.; Lazzaroni, R. *Chem. Mater.* ***1998***, *10*, 4010−4014. (c) Lazzaroni, R.; Leclère, P.; Couturiaux, A.; Parente, V.; François, B.; Brédas, J. L. *Synth. Met.* **1999**, *102*, 1279−1282. (d) Lee, M.; Cho, B.-K.; Oh, N.-K.; Zin, W.-C. *Macromolecules* **2001**, *34*, 1987−1995. (e) Klok, H.-A.; Lecommandoux, S. *Adv. Mater.* **2001**, *13*, 1217−1229.
(14) Thomas, E. L.; Chen, J. T.; O'Rourke, M. J. E. *Macromol. Symp.* **1997**, *117*, 241−256.
(15) (a) Chen, J. T.; Thomas, E. L.; Ober, C. K.; Hwang, S. S. *Macromolecules* **1995**, *28*, 1688−1697. (b) Mao, G.; Ober, C. K. In *Handbook of Liquid Crystals*; Demus, D., Goodby, J., Gray, G. W., Spiess, H.-W., Vill, V., Eds.; Wiley-VCH: Weinheim, 1998; Vol. 3, pp 66−92. (c) Gopalan, P.; Li, X.; Li, M.; Ober, C. K.; Gonzales, C. P.; Hawker, C. J. *J. Polym. Sci., Part A: Polym. Chem.* **2003**, *41*, 3640−3656.
(16) (a) Poser, S.; Fischer, H.; Arnold, M. *Prog. Polym. Sci.* **1998**, *23*, 1337−1379. (b) Mao, G.; Ober, C. K. *Acta Polym.* **1997**, *48*, 405−422.
(17) Schneider, A.; Zanna, J.-J.; Yamada, M.; Finkelmann, H.; Thomann, R. *Macromolecules* **2000**, *33*, 649−651.
(18) (a) Bates, F. S.; Fredrickson, G. H. *Annu. Rev. Phys. Chem.* **1990**, *41*, 525−557. (b) Bates, F. S. *Science* **1991**, *251*, 898−905.
(19) (a) Radzilowski, L. H.; Stupp, S. I. *Macromolecules* **1994**, *27*, 7747−7753. (b) Stupp, S. I.; LeBonheur, V.; Walker, K.; Li, L. S.; Huggins, K. E.; Keser, M.; Amstutz, A. *Science* **1997**, *276*, 384−389. (c) Radzilowski, L. H.; Carragher, B. O.; Stupp, S. I. *Macromolecules* **1997**, *30*, 2110−2119.
(20) Tew, G. N.; Pralle, M. U.; Stupp, S. I. *J. Am. Chem. Soc.* **1999**, *121*, 9852−9866.
(21) Tew, G. N.; Pralle, M. U.; Stupp, S. I. *Angew. Chem., Int. Ed.* **2000**, *39*, 517−521.
(22) Li, W.; Morkved, T. L.; Maddux, T.; Zhu, W.; Jaeger, H. M.; Yu, L. *Polym. Prepr.* **1997**, *38*, 662−663.
(23) Urban, V.; Wang, H. H.; Thiyagarajan, P.; Littrell, K. C.; Wang, H. B.; Yu, L. *J. Appl. Crystallogr.* **2000**, *33*, 645−649.
(24) de Boer, B.; Stalmach, U.; van Hutten, P. F.; Melzer, C.; Krasnikov, V. V.; Hadziioannou, G. *Polymer* **2001**, *42*, 9097−9109.
(25) (a) Stalmach, U.; de Boer, B.; Videlot, C.; van Hutten, P. F.; Hadziioannou, G. *J. Am. Chem. Soc.* **2000**, *122*, 5464−6472. (b) de Boer, B.; Stalmach, U.; Melzer, C.; Hadziioannou, G. *Synth. Met.* **2001**, *121*, 1541−1542.
(26) (a) Nguyen, T.-Q.; Kwong, R. C.; Thompson, M. E.; Schwartz, B. J. *Appl. Phys. Lett.* **2000**, *76*, 2454−2456. (b) Zyung, T.; Jung, S.-D.; Hwang, D.-H. *Synth. Met.* **2001**, *117*, 223−225.
(27) (a) Nguyen, T.-Q.; Doan, V.; Schwartz, B. J. *J. Chem. Phys.* **1999**, *110*, 4068−4078. (b) Nguyen, T.-Q.; Martini, I. B.; Liu, J.; Schwartz, B. J. *J. Phys. Chem. B* **2000**, *104*, 237−255.
(28) (a) Brabec, C. J.; Sariciftci, N. S. In *Semiconducting Polymers:* Chemistry, Physics and Engineering; Hadziioannou, G., van Hutten, P. F., Eds.; Wiley-VCH: Weinheim, 2000; pp 515−560. (b) Brabec, C. J.; Padinger, F.; Hummelen, J. C.; Janssen, R. A. J.; Sariciftci, N. S. *Synth.* Met. **1999**, *102*, 861−864. (c) Cravino, A.; Zerza, G.; Maggini, M.; Bucella, S.; Svensson, M.; Andersson, M. R.; Neugebauer, H.; Brabec, C. J.; Sariciftci, N. S. *Monatsh. Chem.* **2003**, *134*, 519−527.
(29) (a) Geckeler, K. E.; Samal, S. *Polym.* Int. **1999**, *48*, 743−757. (b) Chen, Y.; Huang, Z.-E.; Cai, R.-F.; Yu, B.-C. *Eur.* Polym. J. **1998**, *34*, 137−151.
(30) (a) Kretzschmann, H.; Meier, H. *Tetrahedron Lett.* **1991**, *32*, 5059−5062. (b) Kretzschmann, H.; Meier, H. *J. Prakt. Chem.* **1994**, *336*, 247−254.
(31) Stalmach, U.; de boer, B.; Post, A. D.; van Hutten, P. F.; Hadziioannou, G. *Angew. Chem., Int. Ed.* **2001**, *40*, 428−430.
(32) Audouin, F.; Nuinge, S.; Nuffer, R.; Mathis, C. *Synth. Met.* **2001**, *121*, 1149−1150.
(33) Hawker, C. J. *Macromolecules* **1994**, *27*, 4836−4837.
(34) Prato, M.; Chain Li, Q.; Wudl, F. *J. Am. Chem. Soc.* **1993**, *115*, 1148−1150.
(35) Grösser, T.; Prato, M.; Lucchini, V.; Hirsch, A.; Wudl, F. *Angew. Chem., Int. Ed. Engl.* **1995**, *34*, 1343−1345.
(36) Schick, G.; Hirsch, A.; Mauser, H.; Clark, T. *Chem.—Eur. J.* **1996**, *2*, 935−943.
(37) Nierengarten, J. F.; Eckert, J. F.; Felder, D.; Nicoud, J. F.; Armaroli, N.; Marconi, G.; Vicinelli, V.; Boudon, C.; Gisselbrecht, J. P.; Gross, M.; Hadziioannou, G.; Krasnikov, V.; Ouali, L.; Echegoyen, L.; Liu, S. G. *Carbon* **2000**, *38*, 1587−1598.
(38) Ederlé, Y.; Mathis, C. *Macromol. Rapid Commun.* **1998**, *19*, 543−547.

(39) Beck, M. T.; Mándi, G. *Fullerene Sci. Technol.* **1997**, *5*, 291−310.
(40) Liu, B.; Bunker, C. E.; Sun, Y.-P. *Chem. Commun.* **1996**, 1241−1241.
(41) (a) Bässler, H. *Phys. Status Solidi B* **1993**, *175*, 15−56. (b) Frommer, J. E.; Chance, R. R. In *Encyclopedia of Polymer Science and Enigeering*, 2nd ed.; Mark, H. F., Bikales, N. M., Overberger, C. C., Menges, G., Eds.; Wiley-Interscience: New York, 1986; Vol. 5, p 477.
(42) Stalmach, U.; Schollmeyer, D.; Meier, H. *Chem. Mater.* **1999**, *11*, 2103−2106.
(43) Martens, H. C. F.; Blom, P. W. M.; Schoo, H. F. M. *Phys. Rev. B* **2000**, *61*, 7489−7493.
(44) Luping, Yu.; Bao, Z. *Adv. Mater.* **1994**, *6*, 156−159.
(45) (a) Samorí, P.; Francke, V.; Müllen, K.; Rabe, J. P. *Chem.−Eur. J.* **1999**, *5*, 2312−2317. (b) Jenekhe, S. A.; Chen, X. L. *Polym. Prepr.* **1999**, *40*, 999−1000. (c) Chen, J. T.; Thomas, E. L.; Ober, C. K.; Mao, G.-P. *Science* **1996**, *273*, 343−346.
(46) (a) Meier, H. *Angew. Chem., Int. Ed. Engl.* **1992**, *31*, 1399−1420. (b) Maddux, T.; Li, W.; Yu, L. *J. Am. Chem. Soc.* **1997**, *119*, 844−845.
(47) Grell, M.; Bradley, D. D. C. *Adv. Mater.* **1999**, *11*, 895−905.
(48) Noël, C. In *Handbook of Liquid Crystals*; Demus, D., Goodby, J., Gray, G. W., Spiess, H.-W., Vill, V., Eds.; Wiley-VCH: Weinheim, 1998; Vol. 3, p 93.
(49) Lee, W. A.; Rutherford, R. A. In *Polymer Handbook*, 4th ed.; Brandrup, J., Immergut, E. H., Grulke, E. A., Eds.; Abe, A., Bloch, D. R., Assoc. Eds.; Wiley-Interscience: New York, 1999; Vol. III, p 139.
(50) This high-molecular-weight DEH−PPV ($M_n \sim 90\,000$ g/mol) was prepared by the anionic polymerization of α,α′-dibromo-2,5-di(2′-ethylhexyloxy)xylene as described by: Neef, C. J.; Ferraris, J. P. *Macromolecules* **2000**, *33*, 2311−2314. The synthesis of the monomer was accomplished in two steps from hydroquinone. The hydroquinone reaction with 2′-ethylhexyl bromide (for details of this etherification see ref 51) was followed by a treatment with paraformaldehyde as described by Neef et al. To control the molecular weight, we used 1 mol % of the initiator (method B). The two additional precipitations were from toluene (0.5 wt %) into acetone/methanol (1:1).
(51) Delmotte, A.; Biesemans, M.; Rahier, H.; Gielen, M.; Meijer, E. W. *Synth. Met.* **1993**, *58*, 325−334.
(52) Stalmach, U.; Kolshorn, H.; Brehm, I.; Meier, H. *Liebigs Ann.* **1996**, 1449−1456.
(53) Matyjaszewski, K.; Woodworth, B. E.; Zhang, X.; Gaynor, S. G.; Metzner, Z. *Macromolecules* **1998**, *31*, 5955−5957.

MA035643O